Fast calorimeter on the pure CsI crystals for the modern e^+e^- Super Factories

H. Aihara[1], D. A. Epifanov[2,3], Y. Jin[4], A. A. Osipov[2,3], E. S. Prokhorova[2,3], B. A. Shwartz[2,3], Yu. V. Usov[2], Yu. V. Yudin[2,3]

[1]*The University of Tokyo, 7-3-1 Hongo Bunkyo-ku, Tokyo 113-0033, Japan*
[2]*Budker Institute of Nuclear Physics, 11, Acad. Lavrentieva Pr., Novosibirsk, 630090 Russia*
[3]*Novosibirsk State University, 1, Pirogova str., Novosibirsk, 630090 Russia*
[4]*Hubert Curien Multi-disciplinary Institute, 23 Rue du Loess - BP28, 67037 Strasbourg, France*

E-mail: D.A.Epifanov@inp.nsk.su

(Received March 24, 2019)

Modern high luminosity e^+e^- factories, like Belle II at SuperKEKB or planned Super Charm-Tau factory require fast calorimeters to cope with severe background conditions. The prototype of the fast electromagnetic calorimeter based on pure CsI scintillation crystals, wavelength shifters with the novel nanostructured organosilicon luminophores, and avalanche photodiodes Hamamatsu S8664-55 is discussed. The results of the tests of the basic element of the calorimeter are reported.

KEYWORDS: electromagnetic calorimeter, CsI crystal, silicon avalanche photodiode, nanostructured organosilicon luminophores

1. Introduction

The ultrahigh luminosity e^+e^- factories, like Belle II at SuperKEKB [1, 2], which already started its operation, and planned Super Charm-Tau factory [3] suffer from severe beam background. To cope with the induced pileup noise in the electromagnetic calorimeter fast scintillation crystals are considered as an appropriate option for the calorimeter upgrade/construction [4]. Pure CsI crystals with the scintillation decay time of 30 ns, notable light yield, high radiation hardness, handy mechanical properties and modest price represent attractive variant for the modern calorimetry.

Recently, the counter based on the pure CsI (CsI(pure)) crystal (of $6\times6\times30$ cm^3 size), wavelength shifting (WLS) PMMA plate with the nanostructured organosilicon luminophores (NOL-9) [8, 9], four avalanche photodiodes Hamamatsu APD S8664-55 coupled to the edge sides of the WLS plate, and four-channel charge sensitive preamplifier CAEN A1422B045F3 was studied and the acceptable performance of the counter was demonstrated [5–7]. The specific light output (sLO) of the counter was evaluated to be sLO = (100 ± 10) photoelectrons/MeV, and the equivalent noise energy (ENE) was measured to be ENE = (0.36 ± 0.03) MeV at the shaping time of 30 ns.

The next step towards the construction of the calorimeter prototype was to develop the standard counter: optimize the size and shape of the WLS plate, choose the scheme to couple 4 APDs to the WLS plate, develop four-channel custom-made charge sensitive preamplifier, optimize mechanics of the shielding box.

In this paper we discuss several issues on the construction of the standard counter.

2. Spectral variation of the APD gain and excess noise factor

In the counter based on the CsI(pure) crystal, WLS plate and APD(s) (Hamamatsu S8664-55 or S8664-1010), the stochastic noise, $\sim \sqrt{F/N_{\text{ph.e.}}}$ (determined by the statistics of photoelectrons, $N_{\text{ph.e.}}$,

produced in APD before avalanche gain, and the APD excess noise factor, F) provides notable contribution to the energy resolution of the calorimeter at small energies. Previously, for the Hamamatsu APD S8664-55 (at gain 50) the excess noise factor was measured to be $F = 4.7 \pm 0.5$ for the detected light with the wavelength of $\lambda = 670$ nm [6]. Normally, for the APD gain of 50, F should not exceed factor of 2, determined by the fluctuation of the electron component of the avalanche. Enhanced value of F for the detected light with the wavelength of $\lambda = 670$ nm is associated with the internal geometrical structure of the APD (the depth of the region with the strong electric field is only $3 \div 5\,\mu$m from the APD entrance window) and large photon absorption length in silicon $\ell_\gamma(670\text{ nm}) \approx 3.5\,\mu$m. It became acute to measure the spectral characteristics of APD: gain ($G(\lambda)$), and excess noise factor ($F(\lambda)$) as functions of the wavelength.

The scheme of the setup for the measurement of $G(\lambda)$ and $F(\lambda)$ is shown in Fig. 1. The gain,

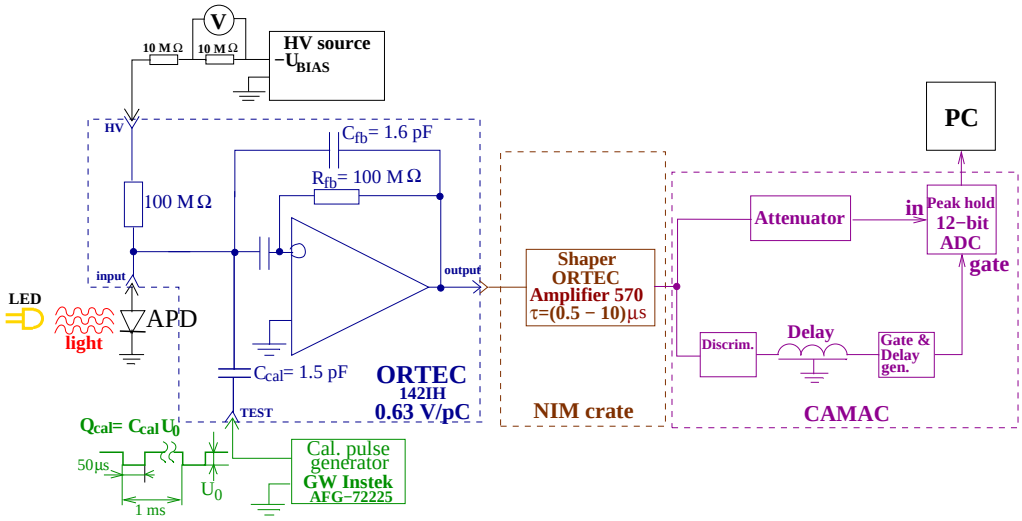

Fig. 1. Experimental setup for analyzing signal from APD.

$G(U_{\text{BIAS}}|\lambda)$, at the APD bias voltage U_{BIAS} and wavelength of the absorbed light λ is measured as a ratio of the APD photocurrents: $G(U_{\text{BIAS}}|\lambda) = \frac{I_{\text{light}}(U_{\text{BIAS}}|\lambda) - I_{\text{dark}}(U_{\text{BIAS}})}{I_{\text{light}}(10\,\text{V}|\lambda) - I_{\text{dark}}(10\,\text{V})} = \frac{I_{\text{photo}}(U_{\text{BIAS}}|\lambda)}{I_{\text{photo}}(10\,\text{V}|\lambda)}$, where $I_{\text{photo}}(10\,\text{V}|\lambda) = I_{\text{light}}(10\,\text{V}|\lambda) - I_{\text{dark}}(10\,\text{V})$ is photocurrent at the $U_{\text{BIAS}} = 10\,\text{V}$ with the unitary gain $G(10\,\text{V}|\lambda) = 1$, $I_{\text{light}}(U_{\text{BIAS}}|\lambda)$ is the total current at the bias voltage U_{BIAS} when the APD is illuminated by the light with the wavelength λ, $I_{\text{dark}}(U_{\text{BIAS}})$ is dark current at the APD bias voltage U_{BIAS}. Six light-emitting diodes (LED) of series ARL-3214 and L-7104UVC were used to provide the light in the range $\lambda = (395 \div 630)$ nm.

To measure the APD excess noise factor $F(\lambda)$ the equivalent noise charge (ENC) in the electronic readout chain was studied for the APD with and without LED illumination, see Fig. 1. Test pulses with constant amplitude, U_0, are fed to the test input of the charge sensitive preamplifier ORTEC 142IH injecting charge $Q_{\text{cal}} = C_{\text{cal}}U_0$, where $C_{\text{cal}} = (1.50 \pm 0.02)$ pF. Voltage signal from the preamplifier is then filtered and amplified by the shaper ORTEC Amplifier 570 and digitized by CAMAC peak hold ADC A0309. The mean value of the peak in the amplitude spectrum is used to graduate ADC channels in the units of incoming charge, and the root mean square (r.m.s.) is a measure of the ENC (we evaluate ENC in the units of electron charge $|e|$). The excess noise factor is calculated from the values of ENC^2 measured with ($\text{ENC}^2_{\text{light}}$) and without ($\text{ENC}^2_{\text{dark}}$) LED illumination: $F(U_{\text{BIAS}}|\lambda) = \frac{|e|[\text{ENC}^2_{\text{light}}(U_{\text{BIAS}}|\lambda) - \text{ENC}^2_{\text{dark}}(U_{\text{BIAS}})]}{2I_{\text{photo}}(U_{\text{BIAS}}|\lambda)G(U_{\text{BIAS}}|\lambda)\tau K_{\text{sh}}}$, where $\tau = 1\,\mu$s is the shaping time, and K_{sh} is a factor determined by the filtering scheme of the shaping amplifier ORTEC Amplifier 570. The K_{sh} was measured with

PIN photodiode Hamamatsu S2744-08 (at the bias voltage of 60 V) instead of APD in the electronic chain: $K_{\rm sh} = \frac{|e|[{\rm ENC}^2_{\rm light} - {\rm ENC}^2_{\rm dark}]}{2I_{\rm photo}\tau} = 1.55 \pm 0.06$.

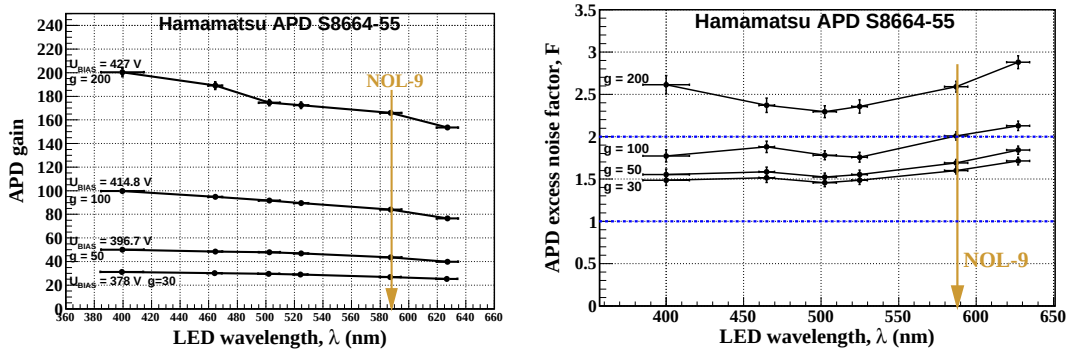

Fig. 2. Hamamatsu APD S8664-55 gain vs. wavelength of the detected light at the constant bias voltage (left), Hamamatsu APD S8664-55 excess noise factor vs. wavelength at the constant APD gain (right).

The Hamamatsu APD S8664-55 gain and excess noise factor as a function of the wavelength are shown in Fig. 2. In Table I we summarize the data on the excess noise factor at the wavelength of 588 nm (maximum of the emission spectrum of NOL-9) at different operating points with gain of 30, 50, 100 and 200 for Hamamatsu APDs S8664-55 and S8664-1010. It is seen that for the nominal

Table I. The excess noise factor, F, at the wavelength of 588 nm for the gains $G = 30,\ 50,\ 100,\ 200$ for Hamamatsu APDs S8664-55 and S8664-1010.

APD type	$F(G = 30)$	$F(G = 50)$	$F(G = 100)$	$F(G = 200)$
S8664-55	1.59 ± 0.04	1.69 ± 0.04	2.00 ± 0.05	2.58 ± 0.06
S8664-1010	1.05 ± 0.02	1.14 ± 0.04	1.37 ± 0.04	2.07 ± 0.05

APD S8664-55 operating point with gain of 50, the excess noise factor for the light reemitted by the WLS plate with NOL-9 is $F(G = 50) = 1.69 \pm 0.04$, which allows us to keep the stochastic noise at the acceptable level.

3. Optimization of the WLS plate

The effect of the shape of the PMMA plate on the light collection efficiency (LCE) was studied without WLS luminophores. The plate with 4 APDs was coupled to CsI(Tl) crystal (of $6\times6\times30$ cm^3 size) and spectrum of the energy deposition from the cosmic particles (having peak of the most probable energy deposition of about 33 MeV) was collected. We monitor the ratio of the cosmic peak positions for the particular type of the plate and the reference one (rectangular plate of $60\times60\times8$ mm^3 size). Plates of several shapes shown in Fig. 3 were tested. The LCE improvement of about 1.6 was observed for the plates 4 and 6. The plate of the type 6 was chosen as the main option once it provides larger sensitive area in the shielding box of the fixed sizes. We also tested the effect of the thickness (8, 12, 16, 20 mm) of the plate 6, the thickness of 8 mm was found to be optimal.

Several types of optical epoxy resin (PEO-210KE, PEO-610KE-20/0, PEO-510KE-20/0, BC600, Polytec) to couple APDs to the edge sides of the PMMA plate were tested. The PEO-210KE, PEO-510KE-20/0 and BC600 showed the highest close to each other LCEs.

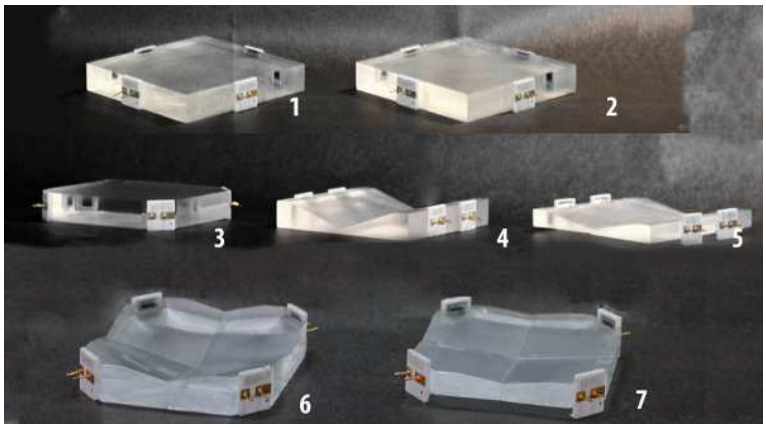

Fig. 3. PMMA plates of different shapes, 1 - reference plate of $60 \times 60 \times 8\,\mathrm{mm}^3$ size.

4. Construction of the first counter

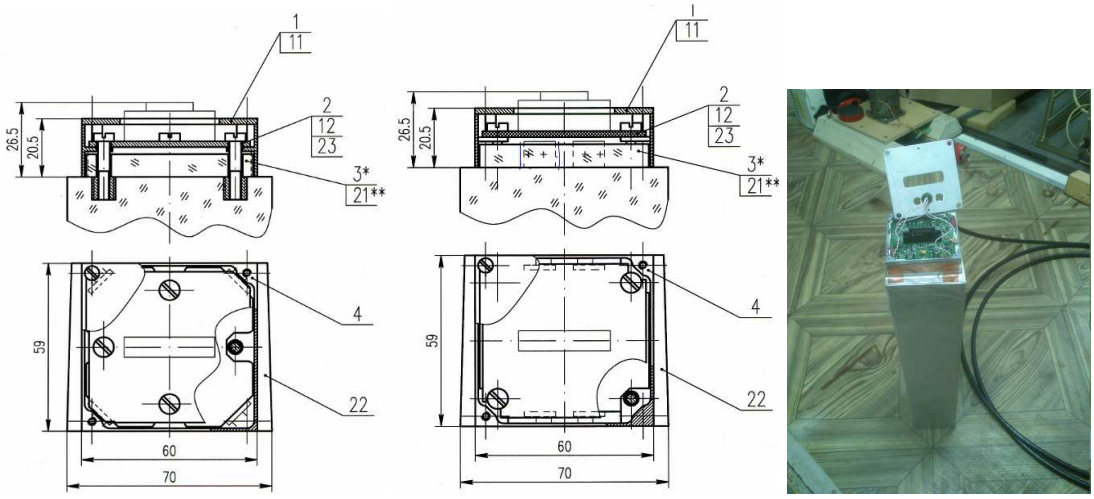

Fig. 4. The first variant of the counter, four APDs are coupled to the truncated corners of the type 3 or 6 plate (left); the second variant of the counter, two pairs of APDs are coupled to the opposite edge sides of the type 4 plate (middle), the photo of the mounted counter of the first variant, the upper lid of the shielding box is opened (right).

Two types of mechanical construction of the counter were tested, see Fig. 4. The first variant is optimized for the usage of the WLS plate of type 3 or 6, while the second variant - for the usage of WLS plate of type 1 and 4. In the aluminium shielding box with fixed sizes, the plate of type 3 or 6 has notably larger sensitive area, hence the signal from the counter of the first variant is larger, we chose this design as a reference, see Fig. 4 (right). In the first counter the WLS plate of type 3 was used. The custom-made four-channel charge sensitive preamplifier was designed on the $53 \times 55\,\mathrm{mm}^2$ PCB. Each preamplifier channel has the sensitivity of 0.2 V/pC with 2 input FET 2SK932, differential output, HV bias circuit and test pulse input. The procedure of the electric mounting of the counter was elaborated. The readout of the signal from the counter was performed by four-channel CAMAC Shaper-ADC board with CR-$(RC)^4$ filter ($\tau = 30\,\mathrm{ns}$), 40 MHz 12-bit pipelined ADC and 256-word circular buffer

for the digitized amplitudes. Amplitude spectrum from cosmic particles for the reference counter is shown in Fig. 5, light output was measured to be sLO = (80 ± 20) photoelectrons/MeV.

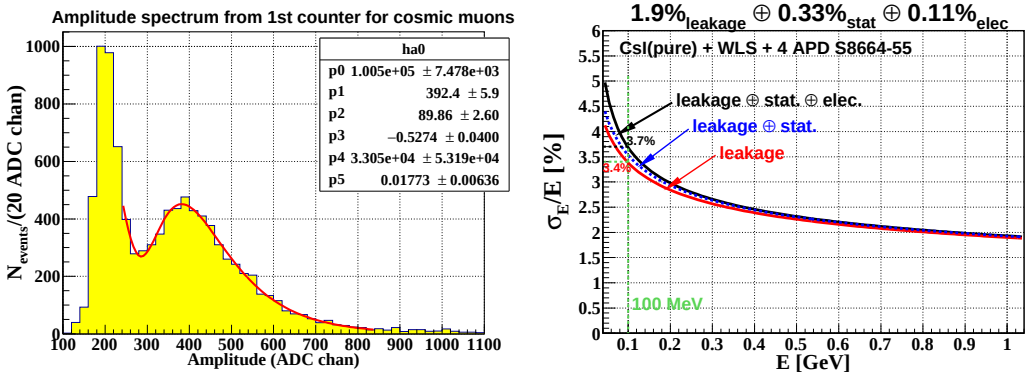

Fig. 5. Amplitude spectrum from cosmic particles for the reference counter (left); the estimated energy resolution of the calorimeter based on the CsI(pure) crystals, WLS(NOL-9) plates and Hamamatsu APDs S8664-55 (right).

5. Conclusion

CsI(pure) inorganic scintillation crystal is an appropriate material for the electromagnetic calorimeter of the modern e^+e^- factories. Compact, insensitive to magnetic field and modest price Hamamatsu APD S8664-55 is an appropriate photosensitive element, several APDs in one counter provide signal readout redundancy. An essential increase (×6 times) of the light output of the CsI(pure)+4APDs counter was achieved with the WLS plate of type 6 made of PMMA and NOL-9, which allows one to construct the calorimeter with high energy resolution of $\sigma_E/E = 3.7\,\%$ for 100 MeV gammas, see Fig. 5 (right). The calorimeter prototype of 16 counters based on CsI(pure) crystals, WLS(NOL-9) plates and Hamamatsu S8664-55 APDs is under construction. All necessary electronics (preamplifiers, Shaper-ADC boards) have been developed and produced. The prototype will be studied on the ROKK [10] test beam facility in 2019 in Budker Institute of Nuclear Physics.

References

[1] T. Abe *et al.* [Belle-II Collaboration], arXiv:1011.0352 [physics.ins-det].
[2] E. Kou *et al.* [Belle II Collaboration], arXiv:1808.10567 [hep-ex].
[3] A. E. Bondar *et al.* [Charm-Tau Factory Collaboration], Phys. Atom. Nucl. **76**, 1072 (2013) [Yad. Fiz. **76**, no. 9, 1132 (2013)].
[4] V. Aulchenko *et al.*, J. Phys. Conf. Ser. **587**, no. 1, 012045 (2015).
[5] Y. Jin, H. Aihara, O. V. Borshchev, D. A. Epifanov, S. A. Ponomarenko and N. M. Surin, Nucl. Instrum. Meth. A **824**, 691 (2016).
[6] H. Aihara, O. Borshchev, D. Epifanov, Y. Jin, S. A. Ponomarenko and N. M. Surin, PoS PhotoDet **2015**, 052 (2016).
[7] H. Aihara, D. Epifanov, Y. Jin and K. Wan, PoS ICHEP **2016**, 703 (2016).
[8] S. A. Ponomarenko, *et al.*, Sci. Rep. 4 6549 (2014).
[9] http://www.luminnotech.com/
[10] G. Y. Kezerashvili, A. M. Milov, N. Y. Muchnoi and A. P. Usov, Nucl. Instrum. Meth. B **145**, 40 (1998).